DESIGN AND TESTING OF LARGE-BORE, ULTRA-STIFF RAILGUNS

J. H. Price, E. P. Fahrenthold, D. R. Peterson, W. F. Weldon,
R. C. Zowarka, Jr., W. G. C. Fulcher, and M. W. Ingram

Presented at the
4th Symposium on Electromagnetic
Launch Technology
Austin, Texas
April 12-14, 1988

Publication No. PR-65
Center for Electromechanics
The University of Texas at Austin
Balcones Research Center
EME 1.100, Building 133
Austin, TX 78758-4497
(512)471-4496

DESIGN AND TESTING OF LARGE-BORE, ULTRA-STIFF RAILGUNS

J. H. Price*, E. P. Fahrenthold**, C. W. G. Fulcher*,
D. R. Peterson*, W. F. Weldon*, and R. C. Zowarka, Jr.*

* Center for Electromechanics, The University of Texas at Austin
10100 Burnet Road, Austin, TX 78758
** Department of Mechanical Engineering, The University of Texas at Austin
Austin, TX 78712

Abstract: Hypervelocity projectile development facilities for armor-antiarmor applications at the Center for Electromechanics at The University of Texas at Austin (CEM-UT) will be expanded with the development of a 90-mm diameter bore, 10-m long electromagnetic railgun and firing-range constructed as part of a program sponsored by the Defense Advanced Research Projects Agency (DARPA) and the U. S. Army Armament Research, Development, and Engineering Center (ARDEC). The railgun in this facility will provide an order-of-magnitude increase in projectile kinetic energy capabilities compared to existing railguns and will be capable of accelerating projectiles to velocities between 2.5 and 4.0 km/s at muzzle energies up to 9 MJ.

In view of the program goals, operational requirements for the facility, and the desire to provide a valid comparison between electromagnetic (EM) and conventional gun technologies, extrapolation of pre-existing railgun designs was avoided in favor of pursuing a systematic design approach targeted at identifying critical gun design constraints affecting hypervelocity projectile performance. Results of the study led to a laboratory-based EM gun design that provides bore straightness and tolerances characteristic of light-gas guns, dynamic bore deformations comparable to those of conventional guns, the ability to quickly change and test rail/sidewall insulator materials, and superior in-bore performance diagnostics.

This paper discusses the railgun design approach, performance parameters, and analytical and empirical railgun structural simulation techniques used to validate the full scale gun design, as well as fabrication status and initial performance test results.

Introduction

As a participant in the DARPA/Army-sponsored EM technology demonstration program, CEM-UT is contracted to provide a laboratory-based EM launcher capable of accelerating armor-penetrating projectiles to velocities between 2.5 and 4.0 km/s at a muzzle energy of 9 MJ [1]. The ability to accelerate projectiles to velocities in this range will provide valuable performance data on flight dynamics and impact mechanics of advanced armor penetrating projectile prototypes.

Critical elements in successful firing of advanced projectiles are the railgun, armature [2], projectile, and sabot. Dynamic interactions of these elements during the launch are closely coupled and poor design of any one could lead to failure of the projectile/sabot/armature package and damage to the bore of the gun. Consequently, projectile and armature design constraints must be considered when addressing the railgun design.

Due to the lack of performance data for railguns operated at energy levels required in this program, some base-line operational parameters for the EM gun were derived from conventional gun performance characteristics. Early in the program, a 90-mm diameter, round gun bore geometry was selected because of the broad base of experience in sabot design for round-bore conventional guns. Peak dynamic bore deformations were to be limited to those in 120-mm tank guns. Finally, to minimize projectile balloting and adverse lateral accelerations, bore straightness and diametral tolerances were based on light-gas gun requirements [3].

The railgun design philosophy that emerged provided an EM launcher that exhibited exceptional structural stiffness and strength, high-precision bore finish and tolerances, infrequent maintenance, and simple maintenance requirements. Solid sliding armatures were selected for improved efficiency and to avoid plasma ablation of bore materials. However, the gun was designed to allow for and seal against plasma armatures in order to provide flexibility during testing.

An isometric section of the final gun design is shown in figure 1. This design consists of three major subsystems; the rail/sidewall insulator package, the rail support structure, and the breech/muzzle connections. In the following sections, a discussion of the issues affecting the gun design is presented and an overview of the composition and operation of the gun components is given along with some insights into the detailed design of the gun.

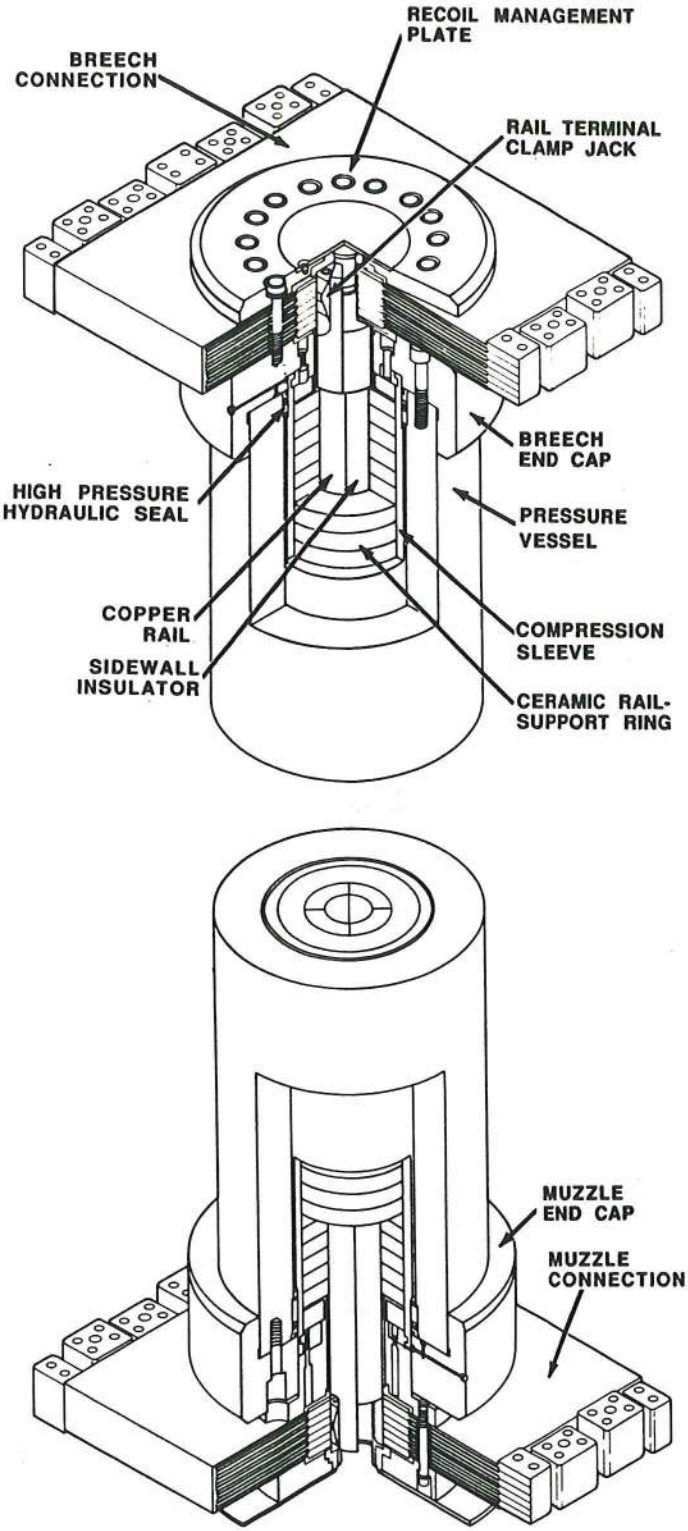

Figure 1. Hydraulically-prestressed railgun

EM Gun Design Issues

Structural design of the EM launcher obviously impacts the ability of the of the device to effectively accelerate a projectile to velocities of interest. Given the nature of the coupled design constraints rising from the severe mechanical and EM loading conditions, a number of novel EM gun structural design concepts have been considered, some of which are shown in figure 2. During the process of evaluating alternate gun structural designs, gun stiffness (defined in the next section) proved to be the key characteristic by which all designs were compared.

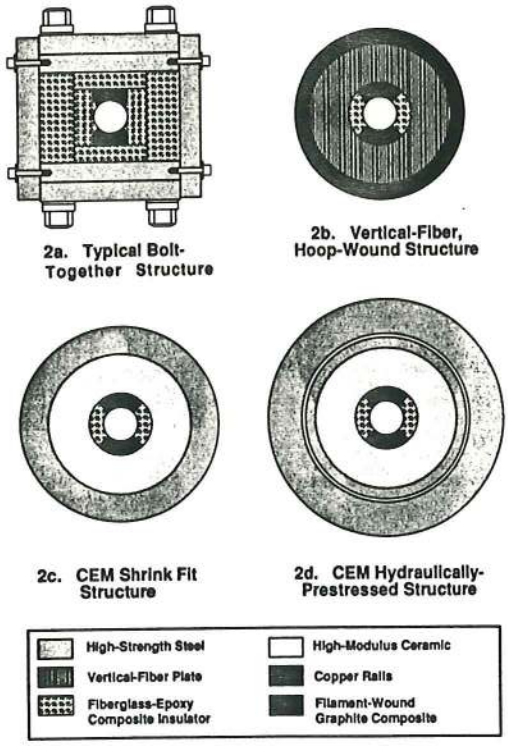

Figure 2. Candidate railgun design cross sections

Gun Stiffness

The term gun stiffness is used here as a quantity representative of the amount of bore deformation a gun structure exhibits in response to an applied EM load. Maximizing gun stiffness, and therefore minimizing bore deformations, can reduce projectile balloting, improve maintenance of solid armature sliding contact, avoid plasma blow-by of the projectile, and prevent rail/insulator seam leakage when using arc-armature drives.

An effective figure-of-merit for comparisons of gun stiffness may be derived by calculating the magnetic "pressure" applied to the rail surface divided by the bore strain. The bore strain is the ratio of rail radial displacement to bore radius. This value may be used as an approximate measure of the effectiveness of candidate designs in minimizing adverse bore deformations. The figure-of-merit is simply

$$M \equiv \frac{P}{(\delta/r)}$$

where

M	≡	gun modulus	[pressure/strain]
δ	≡	rail radial displacement	[length]
r	≡	bore radius	[length]
P	≡	applied pressure	[force/unit area].

To illustrate, M values for various gun designs [4,5,6,7] (including the one presented here) have been calculated and are presented in figure 3. As can be seen, there can be significant differences in the moduli of various designs, where the structures with the highest M values are the most desirable.

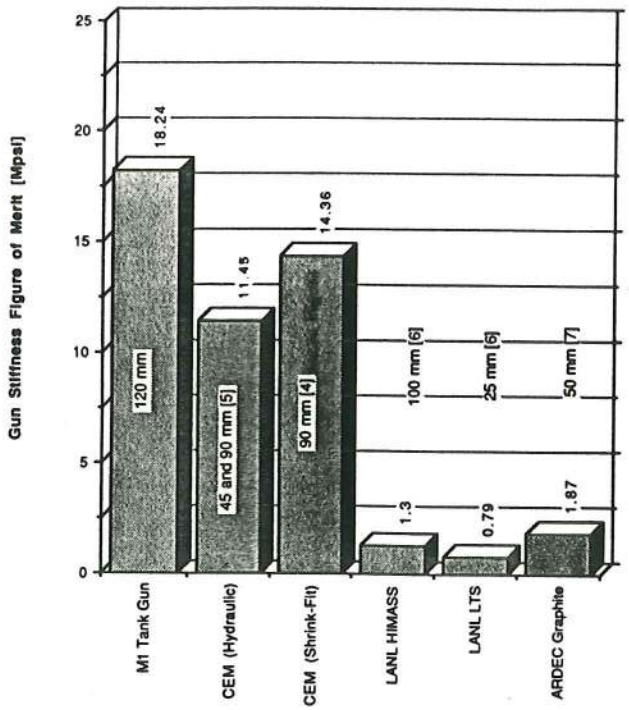

Figure 3. Comparison of gun modulus

During the evaluation process, three general design factors impacted the stiffness of a particular structural design. These parameters were *component material properties, structural prestress of the gun components, and component geometric configuration.*

Component Material Properties

Due to electrical and EM operational constraints, EM gun designers have a limited selection of structural materials at their disposal. Most gun designs to date have utilized high-strength, nonferromagnetic, nonconductive composites as structural materials. Although composite materials exhibit some favorable mechanical properties, effective utilization of composites to provide a stiff gun structure is difficult.

This difficulty arises from the highly anisotropic properties of composite materials. Composite material manufacturers publish unidirectional strengths up to 5,650 MPa (820 ksi) and unidirectional stiffness up to 827 GPa (120 Mpsi) [8] for state-of-the-art (and quite expensive) graphite-fiber materials. However, effective material properties are significantly lower when one includes matrix material properties. Furthermore, volume-fraction effects cause a strength and stiffness reduction when the fibers are cross-plied in a two-dimensional lay-up. An additional reduction in properties results when one considers three-dimensional weaves. Strength reductions arise from low composite strength and stiffness transverse to the fibers, disadvantageous properties in applications that involve triaxial structural loads [9].

In railguns, composites are typically loaded by the rails in a direction transverse to the primary fiber orientation. Therefore, the dominant properties of the composite are effectively those of the matrix material (which can be on the order of 10 or more times less than those in the primary fiber direction). For example, O'Hara and Cascio have shown that for composite-fiber-wrapped railgun structures a factor of five increase in fiber modulus resulted in an increase of only 80% in gun stiffness [7]. Conversely, for isotropic materials, the increase in gun stiffness would be approximately proportional to the material modulus. The results of numerical analyses show that the anisotropic behavior of composites limits their performance in applications that consist of complex, triaxial loading conditions in railguns.

For the structure shown in figure 2b, an improvement in composite structure stiffness was realized over purely hoop-wound fibers by reorienting the primary fiber direction parallel to the direction of the repulsion force between the rails. For the same model geometry, changing the rail support materials to exhibit isotropic properties provided the best stiffness when compared to both of the above composite structural designs.

Therefore, for railgun design, one desires materials with isotropic properties, high strength, and zero apparent electrical conductivity. However, one does not have to sacrifice structural strength for stiffness. High modulus isotropic nonconducting materials may be used to provide superior structural stiffness if properly prestressed to avoid failure when loaded. In other words, by proper selection of materials, stiffness and strength considerations may be separated in order to design effective structural components.

Structural Prestress

Although it has been said that "...the higher the preload, the better the [railgun] design..." [6], the degree of preload is no guarantee of the effectiveness of a gun design. It is conceivable that a gun might be designed with no preload that exhibited significantly greater stiffness than one preloaded to the point of failure. In railgun design, preload (prestress) is useful for two purposes.

First, prestress may be used to bias the operating stress range for a given material. For instance, a railgun structural material may be prestressed to a high state of compression whereby subsequent EM loading will relieve the compressive prestress before the material experiences any tensile stresses. Autofrettage is one prestressing technique utilized extensively in the design of conventional guns [10]. Prestress can also be used to a greater advantage in certain types of materials. For steels, a factor of about two in effective strength may be gained while some ceramics may provide a strength increase of as much as a factor of eight.

Secondly, preload can maintain the geometric configuration of a given structural assembly. For structures that consist of many interdependent components, such as railguns, applied loads may change the contact between adjacent components and therefore adversely affect the structural response. One such critical area of concern is the interface between the rails and sidewall insulators, an area that is required to seal against 50,000 psi plasma pressures. If these seal regions open up, plasma pressure may jet forward of the projectile, thus robbing the system of energy, increasing bore damage, and possibly shorting the rails. In addition, if the prestress of the system is not properly controlled, the sidewalls can be forced into the bore during a shot, thus distorting the bore shape and rendering the launcher useless for multi-shot applications.

In general, preload allows one to more effectively utilize the structural properties of stiff materials and can prevent component interfaces and bore seams from opening. Provided that seams and interfaces do not open up and the structural materials do not fail, preload has a secondary effect on gun stiffness.

Component Geometric Configuration

Interaction between the components used to construct a railgun obviously plays an important role in the overall performance of the gun. The configuration of the components with respect to one another determines their interaction and impacts on gun stiffness. This is most easily seen by comparing the cross sections of several typical gun designs (fig. 2).

A typical bolted-gun design (fig. 2a), constructed primarily of plate materials, places many of the structural components in a geometric configuration such that EM loads applied to the rails must be transferred through insulating plates to a strongback and then to preloading bolts. The result is that the softest components (composite plates) in this arrangement dominate the structural performance of the gun.

Although fiber-wrapped guns eliminate many of the components in a bolted structure, the rails still load the composite transverse to the material fiber direction. Again, the soft region of the structure dominates its performance.

Replacing the composite materials in a cylindrical structural geometry with high modulus ceramic increases the stiffness of the structure, although the geometric configuration is still not ideal. Rail and sidewall materials can play a substantial role in gun stiffness. Utilizing stiff materials in the rail and sidewall region of the gun, and providing a capability to transfer high shear and tensile stresses across the interface between the two, can provide dividends in increasing gun stiffness and reducing gun mass. Implementation of these ideas may be critical to the optimization of field-deployed EM guns.

Laboratory-Based Gun Design

After characterizing the parameters that influence gun design, it remained to settle upon a particular structural geometry and refine the design of its components. The gun design shown in figure 1 was chosen over other candidate gun designs because it exhibited the highest stiffness, provided the ability to easily change the rail and insulator materials, and utilized commercially available materials fabricated with conventional technologies. Because the gun was to be laboratory based, minimizing gun weight was given a low priority. Performance data for a half-scale (45-mm bore) and full-scale (90-mm bore) gun are listed in table 1.

Major subsystems of the launcher include the rail support structure, rail/sidewall insulator package, and the breech/muzzle connection. However, the functionality of the overall design is determined in large part by the rail support structure.

Table 1. Hydraulically prestressed gun; performance data

Parameter	90-mm Dia. Bore	45-mm Dia. Bore
Length	10 m	3 m
Peak Current	3.2 MA	1.6 MA
Inductance Gradient	0.368 μH/m	0.368 μH/m
Muzzle Energy	9 MJ	1.1 MJ
Muzzle Velocity	2.5–4.0 km/s	2.5–4.0 km/s
Bore Magnetic Pressure	54.1 kpsi	54.1 kpsi
Peak Radial Bore Deflection	0.0065 in.	0.0033 in.
Bore Straightness	0.004 in./ft	0.004 in./ft
Bore Roundness	0.004 in.	0.002 in.
Rail Material	AMAX OFHC® Copper	AMAX OFHC® Copper
Sidewall Material	Fiberglass/ Epoxy	Fiberglass/ Epoxy

Rail Support Structure

Two design criteria, high stiffness and easy maintenance, resulted in the rail support structure design eventually chosen. High stiffness was easily provided by the selection of cylindrical rings of high-modulus ceramic to be the basic structural element. Because the ceramics under consideration exhibited a relatively low tensile strength, their utilization required the provision of additional structural elements, which provided a means of prestressing the ceramic to avoid tensile failure upon EM loading of the system.

Two methods of prestressing the rings were analyzed, both of which required the use of an electrically conductive steel tube to contain the rings. Because of ferromagnetic properties and electrical conductivity of steel, placement of steel arbitrarily close to the rails would result in an adverse reduction of the rail inductance gradient (L') [11]. As a result, a study comparing gun stiffness, gun L', ceramic ring manufacturing difficulties, and cost for a given outside diameter was pursued. In the end, the ratio of rail outside diameter to steel tube inside diameter was fixed at 0.438 which resulted in a gun L' of 0.37 μH/m, which is 86% of the L' of a system without a conducting tube. This result was empirically verified by measurements made in full-scale mock-ups of three candidate rail/tube configurations and by measurements of L' in the half-scale gun.

Both shrink-fit and hydraulic prestressing designs were examined for use as the gun structure. The shrink-fit method was pursued initially because it exhibited the highest stiffness of the two options (see Gun Stiffness section) and required the least number of components. A half-scale mock-up of the structure was fabricated and the ceramic disks thermally fitted into a steel tube, allowing enough interference at room temperature to provide adequate prestress. However, experimental results from the half scale mock-up indicated that friction at the ceramic-steel interface and differences in thermal expansion coefficients might make uniform preloading of the stacked ceramic disks very difficult. In recognition of this fact and in the interest of developing a convenient disassembly capability,the alternate hydraulic preloading scheme was chosen.

The hydraulic method, while not quite as stiff as the shrink-fit design, avoided thermal problems and enhanced capabilities to test several candidate rail and insulator materials. The hydraulically prestressed rail support structure assembly consists of five basic components. They are the ceramic disks, a compression sleeve, the pressure vessel, seal-retaining end plates, and high-pressure hydraulic seal groups. Prestressing of the ceramic with this method is accomplished by pumping fluid (glycerin) into an annular void between the compression sleeve and pressure vessel, pressurizing the cavity to 241 MPa (35 kpsi). Applying a high radial pressure to the outside diameter of the compression sleeve and a corresponding radial compressive stress to the outer diameter of the ceramic rings places the inner diameter of the rings in a high state of compression.

Ceramic rings, as opposed to cylinders, were used because of the fabrication problems associated with manufacturing thick sectioned, high-quality ceramics.

As a result, the minimum calculated tangential stress developed in the rings before firing is -563 MPa (-81.7 kpsi), while during firing the maximum tangential stress at the inside diameter of the rings is -224 MPa (-32.5 kpsi) [5]. The maximum stress in the ceramic occurs at a point directly behind the center of the sidewall insulators, while the minimum stress occurs behind the center of the rails. Failure of the ceramic is based on a maximum normal stress criteria.

This structure has an additional advantage in that the system may be conviently pressurized and, in essence, incorporates as a reversible shrink-fit. This is attractive since after the structure is assembled, it may then be pressurized to a low level, inside diameters of the ceramic rings honed to a precise uniform diameter, and a rail/sidewall insulator package inserted into the assembly. After insertion of the package, the system is pumped to full pressure, closing the clearance between the ceramic and rails, resulting in an interference fit between the package and rings. This interference prestresses the rail/sidewall insulator package and insures that there are no gaps between the support structure and the rails.

By simply relieving the system pressure, the rail/insulator package may be extracted and another inserted in the same manner in a matter of hours. Bolted-together guns, on the other hand, must be totally disassembled to perform the same operation. Fiber-wrapped guns typically have no provisions for replacement of rails and insulators.

In this structure, approximately two hundred 41 cm (16 in.) outside diameter, 18 cm (7 in.) inside diameter, 5 cm (2 in.) thick, 276 GPa (40 Mpsi) modulus 90% aluminum oxide ceramic disks (Coors Porcelain AD 90) make up the primary rail support. These disks are placed in a 10 m (394 in.) long, 2.5 cm (1 in.) thick wall, steel compression sleeve. The compression sleeve/disk assembly is then positioned inside the steel pressure vessel. When in place, there is a 1 cm (0.38 in.) annular cavity between the compression sleeve and the 71 cm (28 in.) outside diameter pressure vessel. This cavity is enclosed at either end by a three-part high pressure seal assembly. Finally, steel end plates are bolted to either end of the pressure vessel to retain the hydraulic seals and maintain alignment between the pressure vessel and compression sleeve.

Design of a pressure vessel to operate at these pressure levels can be difficult. A number of components in the structure required careful analysis. Four features of the system proved to be critical to the success of the overall design. These features were the high-pressure hydraulic seals, the pressure port penetration through the pressure vessel wall, the bolt penetrations at the end of the pressure vessel, and selection of a pressure vessel material.

Hydraulic Seals: Sealing against the high pressure fluid in the pressure vessel was accomplished with a three-component seal assembly. The most difficult aspect of sealing was associated with the relative displacement of the pressure vessel with respect to the compression sleeve. Upon pressurization, the pressure vessel grows 0.8 mm (0.03 in.) radially outward while the compression sleeve seal surface grows 0.3 mm (0.01 in.) radially inward. The combined displacement results in the opening of a 1.1-mm gap through which the sealing materials might extrude. The seal components (fig. 4) overcome this problem by incorporating an aluminum antiextrusion ring where the gap occurs. An active polymeric primary seal, Parker Polypak® Type B, bears on and deformes an ultra-high molecular weight polyethylene backup ring in order to force the antiextrusion ring to stay seated against the gap.

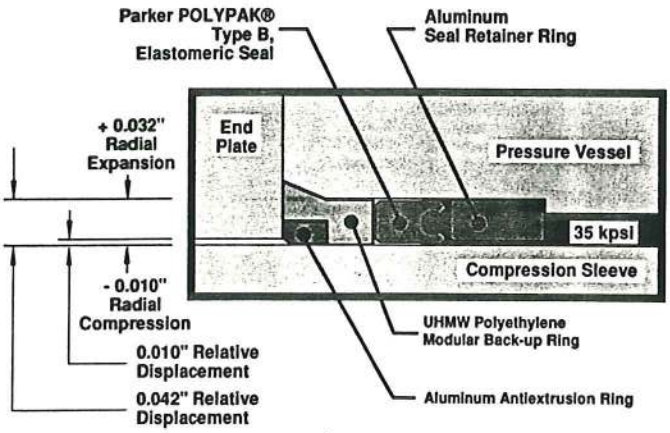

Figure 4. Hydraulic seal group design

Due to Poisson's ratio effects during pressurization, the pressure vessel grows radially outward and shrinks axially while the compression sleeve displaces radially inward and grows axially. If both ends of the components were locked together, large forces (approximately 67 MN (15 Mlb)) would result and consequently fail the sixteen 15 cm (1.5 in.) diameter bolts attaching the end caps to the pressure vessel. This effect was avoided by fixing only the breech end of the tubes together while allowing the muzzle ends to float with respect to each other. The associated relative movement is approximately 2.5 cm (1 in.). The muzzle end seal accommodates this displacement by sliding on the compression sleeve seal surface.

Pressure Port Wall Penetration: The most simple method for providing a penetration in the vessel for the injection of hydraulic fluid was to drill a hole through the wall of the vessel and thread the outside for a high-pressure hydraulic fitting. This simple method introduces a large stress concentration to the highly stressed inside diameter of the pressure vessel. Harvey [12] shows that a cylindrical penetration through the wall of a pressure vessel leads to a stress concentration factor of 2.5 over the nominal stress in the region.

This stress concentration may be reduced, however, by drilling the penetration such that it intersects the bore surface at a 60° angle from a radius and falls within a plane normal to the axis of the tube. This provides an aspect ratio of 2:1 of the major and minor axes of the resultant elliptical penetration, with its major axis parallel to the circumferential direction of the tube, and with a stress concentration of 1.5. One may also depend on some plastic redistribution of stress in the region of the penetration, although additional analyses are required and physical testing should be conducted.

Pressure Vessel Bolt Penetrations: Another highly stressed region in the pressure vessel is the area where the end caps bolt onto the end of the tube. Because the penetrations act to reduce the circumferential strength of the pressure vessel, the region was reinforced by encasing the outer diameter of the tube using a portion of each end cap. The end caps increased the effective wall thickness of the pressure vessel substantially. A three-dimensional, elastic-plastic finite element analysis of the region is in progress to determine the maximum stresses in the area [13,14]. Preliminary two-dimensional analysis indicated that the structure is capable of withstanding the design loads for the system.

Pressure Vessel Fabrication: Sizing of the ceramic disks for stiffness and L' considerations fixed the minimum pressure at which the ceramic ring/compression sleeve assembly had to be prestressed. This pressure, 241 MPa (35 kpsi), determined the minimum size of the pressure vessel for a given material yield strength. After initial sizing of the vessel, a search was conducted to locate vendors capable of fabricating such large components to exacting tolerances. After numerous inquiries, National Forge Company of Irvine, PA was selected.

American Society for Testing and Materials (ASTM) material designation ASTM A 723/723M-86a, Class 4 steel was recomended for use in this application. The material is listed as an alloy steel for forgings for high-strength pressure component applications and is commonly used in the construction of pressure vessels and conventional gun tubes. Compared to AISI 4340, this material exhibits superior fracture toughness and low notch sensitivity for a given yield strength. In addition, the ASTM specification lists all necessary inspection techniques required for acceptance of the finished component.

Two iterations were required to successfully forge an acceptable 10-m long pressure vessel. On the first forging attempted, nondestructive tests indicated an unacceptable flaw in the bore of the rough-machined pressure vessel. Several methods for repairing the flaw were evaluated but none proved satisfactory. National Forge fabricated a second pressure vessel as a replacement for the first.

The second pressure vessel exceeded the ASTM specification for Class 4 material by 11% for the minimum yield and 7% for the ultimate strength. Also, the material exhibited 15% elongation and 52% reduction of area. The compression sleeve was fabricated to Class 3 specifications and also exceeded the minimum allowable material properties.

Rail/Sidewall Insulator Package

The rail/sidewall insulator package is a simple assembly performing four basic functions. First, it carries current from the power supply to the projectile. Secondly, it defines the bore geometry through which the projectile must travel. Next, it must seal against any plasma pressure

developed during a shot, and finally, it provides passages through which in-bore EM diagnostics cabling must pass.

The cross section of the package is cylindrical, with the outside diameter equal to twice the bore diameter. The rails and sidewalls are all 90° arc segments. AMAX Copper, Inc. Type OFHC® copper extrusions were used as the stock material for the rails, and E-glass filament-wound tubes utilizing a polyester resin matrix were used as the stock materials for the sidewalls. Three 120° segments were cut from a filament-wound tube to produce three sidewalls.

After the stock materials were produced, the inner radius and orthogonal faces of each component were machined. Troughs (or slots) were machined in the back surfaces of the sidewall insulators to contain magnetic probe cables. Also, a flat surface was machined on the back side of the rails to provide an external reference to the exact position of the bore for future assembly operations. Once machined, the rails and insulators were cleaned and primed to aid bonding of the components with an American Cyanamid FM 123 sheet adhesive. The sheet adhesive was applied to the flat sidewall faces before final assembly.

Final assembly of the package is to be performed in a rigid assembly fixture (fig. 5) that was machined straight to within 0.13 mm (0.005 in.) along its entire length. Individual clamps are piloted onto a reference feature machined into the assembly fixture. These clamps locate the reference surfaces machined on the back sides of the rails, with respect to the assembly fixture, in order to to insure straightness of the assembly after gluing. In addition, a polished mandrel is to be placed inside the rails and insulators during gluing to aid in maintaining bore straightness and insuring bore cylindricity.

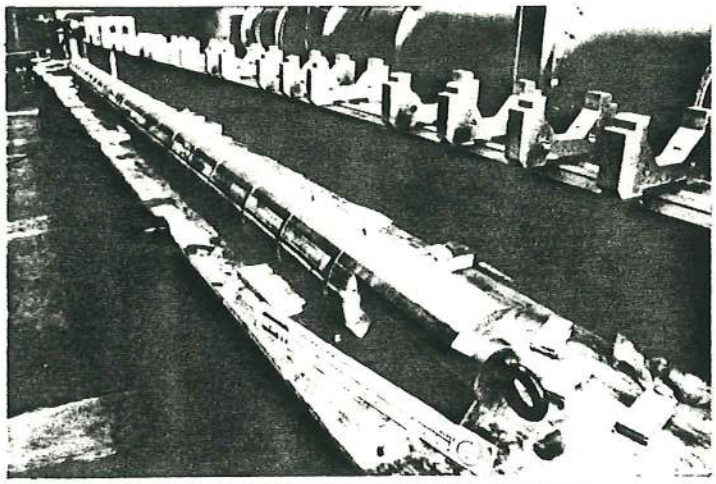

Figure 5. Rail/sidewall insulator package assembly fixture with full-scale rail/sidewall package test assembly

After the rails and sidewalls are clamped into position, the entire assembly is heated to 120° C (250° F) for six hours. Upon curing the sheet adhesive, the assembly is allowed to cool. Afterwards, magnetic probes are installed in the sidewalls with their wires strung to the breech of the gun through troughs located in the back of the sidewalls. With the instrumentation leads in place, the voids in the sidewalls are filled with fiberglass and epoxy. With the instrumentation potted in place, the assembly is sent out for final machining. In the final machining process, the outside diameter of the assembly is turned and the end features on the rails are milled.

The 10-m rails and insulators are in the assembly stage of fabrication. However, a half-scale assembly has been fabricated and is shown in figure 6. Fabrication of the half-scale assembly proved invaluable in guiding development of the assembly techniques required for the full-scale gun.

Breech/Muzzle Connection

Conduction of 3.2 MA into the terminals of any railgun is a difficult task. Given all the fabrication steps required for the rail/sidewall insulator assembly, the addition of a complicated terminal configuration was undesirable. Also, making the geometric transition from the low-inductance, low-pressure buswork of the power supply to the high-inductance, high-pressure rails in the gun introduced significant structural concerns associated with the breech/muzzle connection design. In response to these concerns, the connection configuration shown in figure 7 was designed.

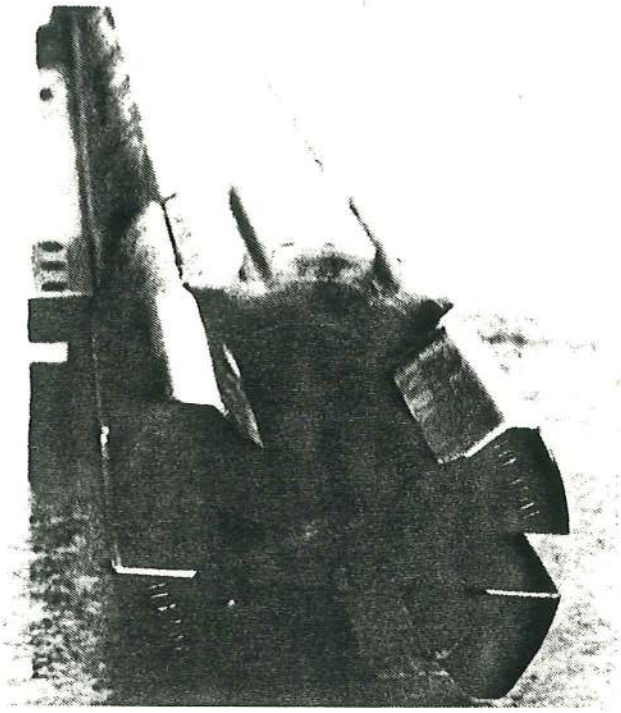

Figure 6. Half-scale rail/sidewall insulator package breech-end terminals

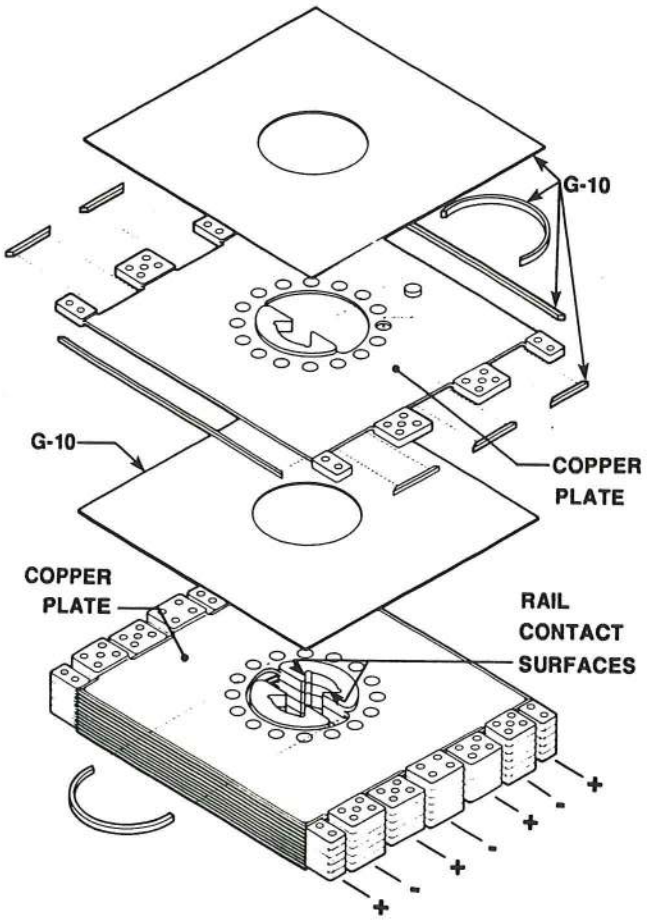

Figure 7. Breech/muzzle connection assembly order

The connection design shown is mechanically self-supporting, makes the transition from our low-inductance bus to the high-inductance rails, is insulated to 25 kV, connects to simple features machined on the rail terminals, leaves the breech open and accessible at all times, and effectively manages gun recoil. The connection consists of 12 laminated conductors, of which six are positive and six are negative, with G-10 insulating sheets between each conductor.

Assembly of the breech connection is accomplished by applying a layer of American Cyanamid sheet adhesive between each layer in the system. This sheet adhesive provides a tensile bond strength of up to 25.6 MPa (4 kpsi). Where bolts are to penetrate the assembly, G-10 disks are placed in predrilled holes in the conducting plates, and G-10 strips are placed around the edges of the conductors to cover any exposed surfaces and block line-of-sight tracking across surfaces. An alignment fixture is used to precisely align the plates during oven-curing of the assembly. After curing, the surfaces that contact the rails are finish-machined and the thru-bolt penetrations are drilled in the proper locations. Afterwards, the assembly is tested with high voltage to insure that the insulation system does not break down and the connection is ready for installation onto the gun.

Repulsion loads are developed within the connection when current flows through the conductors. In the laminated region, the current is distributed over the surfaces of the conductors and results in a low plate-to-plate repulsion force of 2 MPa (300 psi). Where the current transitions from the laminated plates to the parallel rails, the repulsion force rapidly approaches that of the rails and must be supported. The connection was designed such that the full rail repulsion load could be radially applied to the structure and be fully supported by the connection. Because the plates in the system are bonded together, they act as a continuous ring with inner and outer dimensions corresponding to the geometry defined by the laminated plates.

A total recoil force of 2 MN (450 klb) is developed by the 10-m gun during firing. Since recoil in the gun is developed in the EM breech closure of the gun [15], the breech connection, being this closure, was designed to transmit the recoil force to gun structure and thus to ground. Recoil is transmitted from the breech connection to a steel recoil plate and then to bolts that connect the recoil plate to the gun structure, passing through insulated penetrations in the breech connection.

Connection to the rails is accomplished after the rails and insulators are inserted into the gun structure. The breech connection is lowered over the rail terminals until it rests on the breech end plate (fig. 8). A double-wedge jack (fig. 9) is placed in a slot in the end of the rails which, upon tightening, forces the rail terminals out against the contact surfaces on the breech connection. A contact pressure of 103 MPa (15 kpsi) is applied in this manner.

Where the breech connection joins the bus from the power supply, 14 terminals of alternating polarity maintain the low inductance features of the buswork. Since current to the breech is fed symmetrically to each side of the connection, uniform current distribution to the rails is insured.

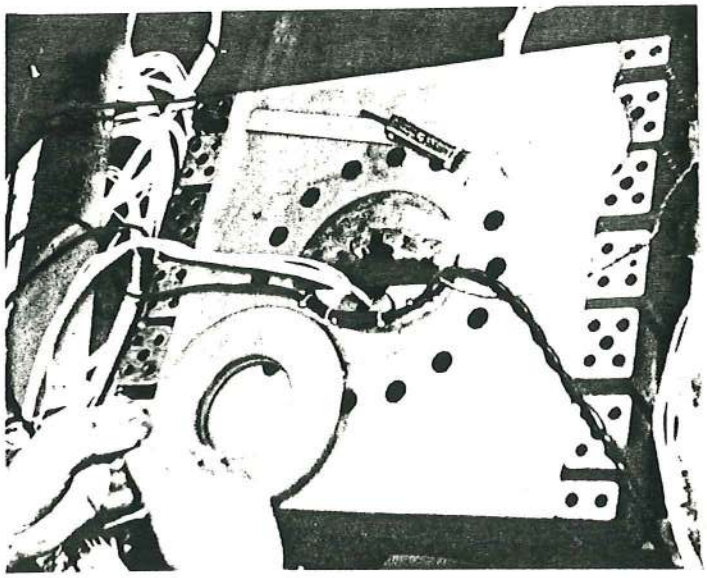

Figure 8. Half-scale breech connection during installation gun structure

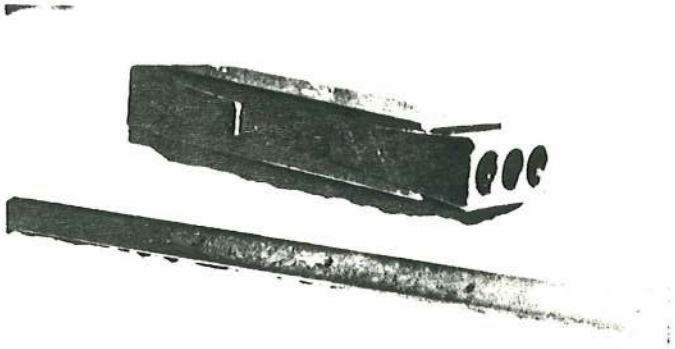

Figure 9. Double-wedge rail terminal clamp jack

Although the preceding discussion considers the connection for the breech end of the gun, the same design is directly applicable as a closing switch connection placed at the muzzle end of the gun. By placing closing switches (crowbars) at the muzzle, tip-off of the projectile upon exit of the gun may be eliminated and erosion damage due to arcing on projectile exit may be reduced.

Test Results and Fabrication Status

As mentioned earlier, an exact half-scale prototype of the gun design under discussion has been fabricated, tested, and is now being used to fire half-scale armatures in the firing range. The half-scale rail support structure has been successfully pressure tested up to 276 MPa (40 kpsi) with all critical stress areas strain-gaged to verify analytical predictions of structural performance.

To date, 11 shots have been fired [1] in the half-scale gun (Fig. 10), at a maximum current of 1.3 MA, with the design current set at 1.6 MA. Routing of the in-bore magnetic probe leads parallel to the rails and thus in the highest transient magnetic field region of the gun was initially viewed as highly undesirable, although experience has shown that doing so has had virtually no impact on the integrity of the signals. Performance of the probes has been remarkable and has provided valuable data as to the in-bore performance of half-scale armatures now being tested. Armature velocities up to 2 km/s have been recorded with in-bore damage being minimal. Between shots, 0.1 mm (0.004 in.) is honed from the diameter of the gun to bring it back to ideal surface conditions. Note that this change in bore dimension is due primarily to an inability to take off any less material in a single honing operation, with actual bore wear somewhat less.

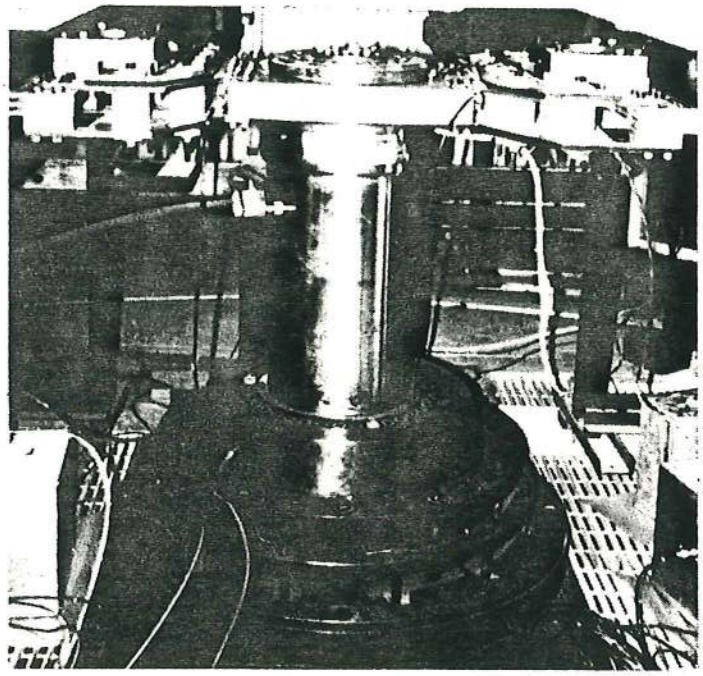

Figure 10. Half-scale gun ready for firing

At the time of this writing, all components of the full-scale gun have been fabricated and received. Both the rail and insulator package and the breech connection assembly are in the final assembly stage. Firing of the half-scale gun is scheduled to proceed through mid-April, 1988. Afterwards, the half-scale gun will be decommissioned and the full-scale gun installed. The first shot of the full-scale gun is scheduled for the latter part of May, 1988.

Conclusions

Analyses performed to evaluate several candidate gun structural concepts have led to a laboratory based EM gun design that satisfies the design goals set forth at the beginning of the program. A high-stiffness, easily maintained, precision-bore 9-MJ EM launcher has been designed and fabrication is virtually complete. A half-scale prototype of this hydraulically-prestressed EM gun design has been fabricated and successfully tested.

General design criteria for optimizing gun stiffness have been developed which appear to be valid for both laboratory-based and field-deployed EM guns. These criteria show that proper utilization of high-modulus materials, proper configuration of components, and prestressing are required to maximize gun stiffness.

Acknowledgments

Research funding for this program was provided by DARPA and ARDEC under contract number DAAA 21-86-C-0215.

References

[1] R. C. Zowarka, Jr., D. R. Peterson, J. H. Price, and W. F. Weldon, "9 MJ Laboratory Gun Range at The University of Texas at Austin," paper presented at the 4th Symposium on Electromagnetic Launch Technology, Austin, TX, April 12-14, 1988.

[2] J. H. Price, J. A. Pappas, C. W. G. Fulcher, M. Ingram, D. Perkins, D. R. Peterson, and R. C. Zowarka, "Design and Testing of Solid Armatures for Large-Bore Railguns," paper presented at the 4th Symposium on Electromagnetic Launch Technology, Austin, TX, April 12-14, 1988.

[3] H. F. Swift, D. E. Strange, and M. Nagy, "The Kinematic Bore Geometry Gage, A New Method for Evaluating Launch Tubes," paper presented at the 37th meeting of the Aeroballistic Range Association, Quebec, Canada, September, 1986.

[4] E. P. Fahrenthold, J. H. Price, and D. R. Peterson, "Structural Design of Cylindrical Railguns," paper presented at the 4th Symposium on Electromagnetic Launch Technology, Austin, TX, April 12-14, 1988.

[5] E. P. Fahrenthold, "Design of Pressure Vessel Cascades for Electromagnetic Launchers," submitted for publication at the ASME Pressure Vessels and Piping Conference, Pittsburg, PA, June 1988.

[6] R. F. Davidson, W. A. Cook, D. A. Rabern, and N. M. Schnurr, "Predicting Bore Deformations and Launcher Stresses in Railguns," IEEE Transactions on Magnetics, vol. MAG-22, no. 26, November 1986, pp 1435-1440.

[7] G. P. O'Hara and M. Cascio, "Structural Integrity of Metallic Armature Railguns," proceedings of the Fifth U. S. Army Symposium on Gun Dynamics," Rensselaerville, NY, September 23-25, 1987.

[8] Amoco Performance Products Data Sheet Numbers F-7055 and F-7027.

[9] R. M. Jones, Mechanics of Composite Materials, McGraw-Hill Book Company, New York, NY, 1975, pp 35-91.

[10] U. S. Army Material Command (AMC), "Research and Development of Materiel, Engineering Design Handbook, Gun Series, Gun Tubes," AMC Pamphlet AMCP 706-252, February 1964.

[11] J. A. Leuer, "Electromagnetic Modeling of Complex Railgun Geometries," IEEE Transactions on Magnetics, vol. MAG-22, no. 26, November 1986, pp 1584-1590.

[12] J. F. Harvey, Theory and Design of Pressure Vessels, Van Nostrand Reinhold Company, Inc., New York, NY, 1985, pp 382-386.

[13] Hibbitt, Karlsson and Sorensen, Inc., ABAQUS User's Manual, Version 4-5.

[14] E. P. Fahrenthold, J. H. Price, and C. W. G. Fulcher, "Stress Analysis of Cylindrical Pressure Vessels With Bolted End Connections," in preparation.

[15] W. F. Weldon, M. D. Driga, and H. H. Woodson, "Recoil in Electromagnetic Railguns," IEEE Transactions on Magnetics, vol. MAG-22, no. 26, November 1986, pp 1808–1811.